Loss of histone methyltransferase Ezh2 stimulates an osteogenic transcriptional program in chondrocytes but does not affect cartilage development

Received for publication, June 11, 2018, and in revised form, October 12, 2018 Published, Papers in Press, October 16, 2018, DOI 10.1074/jbc.RA118.003909

Emily T. Camilleri[‡1], Amel Dudakovic[‡], Scott M. Riester[‡], Catalina Galeano-Garces[‡], Christopher R. Paradise[‡§], Elizabeth W. Bradley[‡], Meghan E. McGee-Lawrence[¶], Hee-Jeong Im[‖], Marcel Karperien[**], Aaron J. Krych[‡], Jennifer J. Westendorf[‡ ‡‡], A. Noelle Larson[‡], and Andre J. van Wijnen[‡ ‡‡2]

*From the Departments of [‡]Orthopedic Surgery, [§]Molecular Pharmacology and Experimental Therapeutics, and [‡‡]Biochemistry and Molecular Biology, Mayo Clinic, Rochester, Minnesota 55901, the [¶]Department of Cellular Biology and Anatomy, Medical College of Georgia, Augusta University, Augusta, Georgia 30912, the [‖]Jesse Brown Veterans Affairs Medical Center, Chicago, Illinois 60612, and the **Department of Developmental BioEngineering, University of Twente, 7522 NB Enschede, The Netherlands*

Edited by Joel M. Gottesfeld

Ezh2* is a histone methyltransferase that suppresses osteoblast maturation and skeletal development. We evaluated the role of *Ezh2* in chondrocyte lineage differentiation and endochondral ossification. *Ezh2* was genetically inactivated in the mesenchymal, osteoblastic, and chondrocytic lineages in mice using the *Prrx1-Cre*, *Osx1-Cre*, and *Col2a1-Cre* drivers, respectively. WT and conditional knockout mice were phenotypically assessed by gross morphology, histology, and micro-CT imaging. *Ezh2*-deficient chondrocytes in micromass culture models were evaluated using RNA-Seq, histologic evaluation, and Western blotting. Aged mice with *Ezh2* deficiency were also evaluated for premature development of osteoarthritis using radiographic analysis. *Ezh2* deficiency in murine chondrocytes reduced bone density at 4 weeks of age but caused no other gross developmental effects. Knockdown of *Ezh2* in chondrocyte micromass cultures resulted in a global reduction in trimethylation of histone 3 lysine 27 (H3K27me3) and altered differentiation *in vitro*. RNA-Seq analysis revealed enrichment of an osteogenic gene expression profile in *Ezh2*-deficient chondrocytes. Joint development proceeded normally in the absence of Ezh2 in chondrocytes without inducing excessive hypertrophy or premature osteoarthritis *in vivo*. In summary, loss of *Ezh2* reduced H3K27me3 levels, increased the expression of osteogenic genes in chondrocytes, and resulted in a transient post-natal bone phenotype. Remarkably, *Ezh2* activity is dispensable for normal chondrocyte maturation and endochondral ossification *in vivo*, even though it appears to have a critical role during early stages of mesenchymal lineage commitment.

Epigenetic regulation of gene expression directs and maintains cellular phenotypes. Mechanisms of epigenetic regulation include post-translational modification of histones (*e.g.* methylation or acetylation), DNA methylation, and both small and long noncoding RNAs. Epigenetic signaling mechanisms are both dynamic and reversible, which makes them attractive targets for therapeutic drug discovery (1). Many different classes of epigenetic regulators, which include polycomb proteins and histone deacetylases, are required for normal skeletal development and differentiation of bone and cartilage (2–13). Therefore, studies of these proteins may lead to novel pharmacological strategies for the treatment of musculoskeletal disorders and injuries, including osteoporosis, osteoarthritis, scoliosis, and fractures, and would complement current cell-based strategies for musculoskeletal tissue regeneration (3, 14, 15).

Normal skeletal development requires the direct and coordinated differentiation of mesenchymal progenitor cells. In early skeletogenesis, mesenchymal progenitors may differentiate into chondrocytes and later form bone through endochondral ossification. Alternatively, they may differentiate into osteoblasts directly through the process of intramembranous bone formation. Mechanisms regulating differentiation include the expression of lineage-specific transcription factors (*e.g.* SOX9 and RUNX2) as well as autocrine or paracrine growth factor signaling (*e.g.* transforming growth factor β (TGF-β), bone morphogenic protein (BMP), wingless/integrated (WNT) (16). Recent studies have also identified epigenetic processes, including histone acetylation and methylation, that contribute to the regulation of differentiation and maturation of mesenchymal progenitors, chondrocytes, and osteoblasts (17–24).

The regulation of histone acetylation and methylation states has also been shown to control chondrogenesis (21, 25–27). Histone deacetylases, which remove acetyl groups from lysines,

This work was supported by NIAMS, National Institutes of Health Grants R01 AR049069 (to A. J. v. W.), R03 AR066342 (to A. N. L.), F32 AR066508 (to A. D.), K01 AR065397 (to E. W. B.), and R01 AR068103 (to J. J. W.) as well as by intramural grants from the Center for Regenerative Medicine at the Mayo Clinic and Mayo Graduate School (Clinical and Translational Sciences Track) and the Center for Clinical and Translational Science (UL1 TR000135). We also appreciate generous philanthropic support from William H. and Karen J. Eby and the charitable foundation in their name. A. J. K. is a paid consultant for Arthrex, Inc., and M. K. is a founder and chair holder of Hy2Care B.V. The content is solely the responsibility of the authors and does not necessarily represent the official views of the National Institutes of Health.

This article contains Figs. S1 and S2 and Tables S1–S3.

The RNA-Seq data have been deposited in the publicly available Gene Expression Omnibus (GEO) repository with accession number GSE97118.

[1] Present address: Masonic Cancer Center, University of Minnesota, Minneapolis, MN 55455.

[2] To whom correspondence should be addressed: Dept. of Orthopedic Surgery, Medical Sciences Bldg., Rm. 3-69, Mayo Clinic, 200 1st St. SW, Rochester, MN 55905. Tel.: 507-293-2105; Fax: 507-284-5075; E-mail: vanwijnen.andre@mayo.edu.

modulate proliferation, hypertrophy, and Wnt signaling pathways in chondrocytes (8, 21). Histone methylation at H3 lysine 9 (H3K9) regulates growth plate development and hypertrophic differentiation (28, 29), whereas inactivation of the histone 3 lysine 27 (H3K27) demethylase enzyme *Jmjd3* (*Kdm6b*) inhibits endochondral bone formation (27).

Previous studies have identified the histone methyltransferase enzyme enhancer of zeste homolog 2 (*EZH2*) as an important regulator in bone development and osteoblast differentiation (2, 4, 30). *EZH2* is the catalytic domain of the Polycomb repressive complex 2 (PRC2) and functions to trimethylate H3K27 (H3K27me3),[3] resulting in chromatin compaction to repress gene expression during skeletal development (3, 31, 32). Global knockout of *Ezh2* in mice is embryonic lethal and results in excessive accumulation of mesoderm cells in abnormal embryos (33). Conditional knockout studies of *Ezh2* in the mesenchymal linage using the *Prrx1-Cre* driver revealed numerous skeletal abnormalities, including shortened limb segments, reduced vertebral height, and premature fusion of the cranial sutures (2, 4, 30). Similarly, conditional inactivation of *Ezh2* in neural crest–derived cartilage modulated *Hox* gene expression and resulted in craniofacial defects in mice (10). These studies suggest that *Ezh2* inactivation affects both endochondral and intramembranous bone formation. In this study, we conditionally inactivated *Ezh2* in chondrocytes using the *Col2a1*-driven *Cre* recombinase to further define the role of *Ezh2* during endochondral ossification.

Results

Ezh2 inactivation does not lead to skeletal defects in lineage-committed cells

Our previous work demonstrated that *Ezh2* inactivation in mesenchymal progenitors (*Prrx1-Cre*) leads to skeletal malformations, in part because of reduced growth plate height and epiphyseal area (2). To evaluate whether Ezh2 deficiency also impacts skeletal development in linage-committed cells, we utilized the cartilage *Col2a1-Cre* driver and bone *Osx1-Cre* driver (Fig. 1*A*). Histological analysis of the proximal tibia of early adolescent (3–4 weeks of age) animals revealed that *Ezh2*-cKO_{OSX} and *Ezh2*-cKO_{Col2} mice did not exhibit changes in cartilage morphology or growth plate depth compared with the respective WT-*Cre*+ animals (Fig. 1, *B–D*).

To validate *Ezh2* inactivation, H3K27me3 and *Ezh2* were measured by IHC in the proximal tibia from post-natal day 1 mice. *Ezh2* and H3K27me3 were observed in the resting zone and hypertrophic chondrocytes of *Ezh2*-WT_{Col2} mice; however, *Ezh2*-cKO_{Col2} animals showed reduced nuclear staining of both H3K27me3 and *Ezh2* Fig. 2*A*).

The development of mice with cartilage-specific inactivation of *Ezh2* was also measured on postnatal day 1 and at 4 weeks and 8 weeks of age. The overall growth, stature, limb length, and weight of cKO_{Col2} mice were similar to control *Ezh2*-WT_{Col2} mice, and no sex-specific differences in these parameters were observed (Fig. 2, *B* and *C*). Together, these results indicate that *Ezh2* is not essential for skeletal development in precommitted chondrocytes and osteoblasts compared with uncommitted mesenchymal progenitors.

Bone quality is reduced in Ezh2 cKO_{Col2} adolescent mice but normalized by adulthood

During the process of endochondral ossification, cartilage forms the framework for ossification by osteoblasts. To evaluate whether *Ezh2* inactivation in chondrocytes affects matrix production and mineralization, we evaluated bone parameters in the proximal tibial metaphysis at 4 weeks and 8 weeks as well as L5 vertebrae at 24 weeks of age. At 4 weeks of age, cKO_{Col2} mice exhibited a 50% reduction in bone volume/tissue volume (BV/TV) compared with control animals, as well as reduced trabecular number (Tb.N) and trabecular thickness (Tb.Th) and increased trabecular spacing (Tb. Sp) (Fig. 3, *A* and *B*, and Table S1). Interestingly, cancellous bone parameters were not different between WT and cKO_{Col2} mice at 8 and 24 weeks of age. These data indicate that chondrocyte-specific deletion of *Ezh2* reduces bone density in young mice, but this phenotype resolves during adulthood.

Transcriptome profiling of immature mouse chondrocytes shows enhanced osteogenic potential of Ezh2 cKO_{Col2} animals

To characterize the chondrocyte-specific *Ezh2* inactivation, we differentiated immature mouse chondrocytes (IMCs) from WT and cKO_{Col2} *ex vivo* for up to 14 days in micromass cultures (Fig. 4*A*). On day 3, the recombination event results in a reduction of Ezh2 exon counts, but a more robust loss in exon counts is observed across exons that encode the Ezh2 SET domain Fig. S1). Similar trends were also observed on days 7 and 14 (data not shown). The expression of *Ezh2* protein as well as H3K27me3 was reduced in cKO IMC cultures on days 3 and 7 (Fig. 4*B*), further demonstrating inactivation of *Ezh2* in chondrocytes. A minor increase in Ezh2 and H3K27me3 levels was observed in hypertrophic chondrocytes (day 14) in cKO IMC cultures that may be attributable to preferential proliferative expansion of cells with nonrecombined Ezh2 alleles. Histological analysis revealed that both cultures formed a hypertrophic chondrocyte-like phenotype, but staining for proteoglycans present in the extracellular matrix was reduced in cKO micromasses compared with those from WT mice Fig. 4*C*). Thus, loss of Ezh2 results in changes in the properties of the chondrocyte-related extracellular matrix *ex vivo*.

We also performed whole-transcriptome analysis of IMC cultures from WT or cKO mice using RNA-Seq to determine the effect of *Ezh2* inactivation in chondrocytes. Unsupervised hierarchical clustering analysis of genes expressed in any of the samples (19,641 of 23,359 genes) revealed distinct clustering of samples according to time point, where day 14 samples form a distinct outgroup (Fig. 4*D*). In particular, IMC cultures from both genotypes differentiated toward the hypertrophic chondrocyte phenotype as indicated by down-regulation of the extracellular matrix proteins *Col2a1* and *Acan* and the transcription factor *Sox9* (Fig. 4*E*). Conversely, the hypertrophy-associated extracellular matrix proteins *Col10a1* and *Vegfa*

[3] The abbreviations used are: H3K27me3, histone H3 lysine 27 trimethylation; IHC, immunohistochemistry; cKO, conditional knockout; BV, bone volume; TV, tissue volume; Tb.N, trabecular number; Tb.Th, trabecular thickness; Tb.Sp, trabecular spacing; IMC, immature mouse chondrocyte; RPKM, reads per kilobase per million; micro-CT, micro-computed tomography.

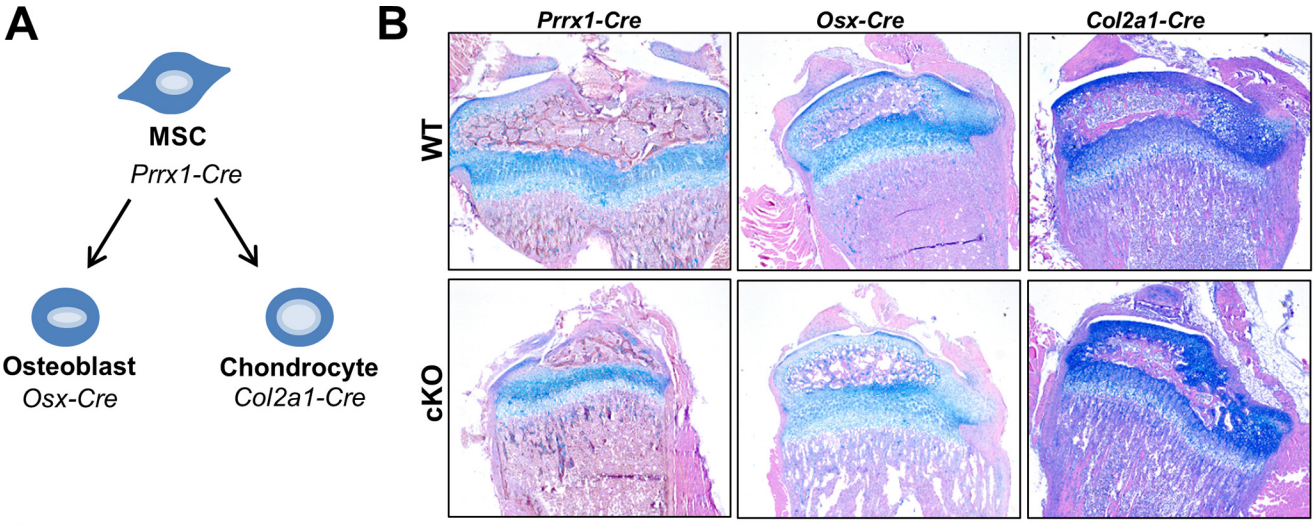

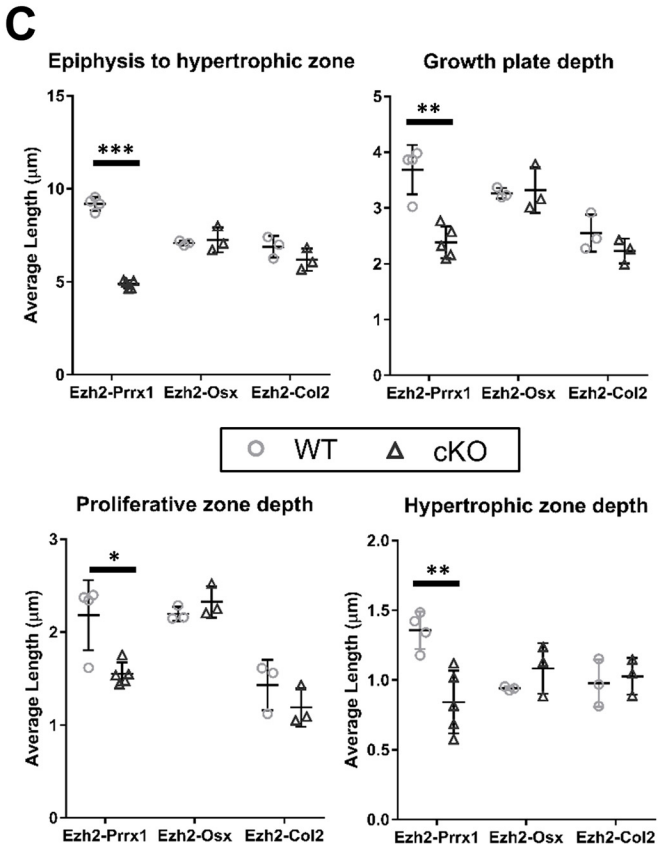

D

Histological assessment of proximal tibia epiphysis and growth plate						
	Ezh2-Prrx1		Ezh2-Osx		Ezh2-Col2	
	WT	cKO	WT	cKO	WT	cKO
Epiphysis to hypertrophic zone	9.19 (0.36)	4.88 (0.21)	7.08 (0.13)	7.26 (0.66)	6.89 (0.58)	6.19 (0.59)
	p=0.000006		p=0.6949		p=0.2200	
Growth plate depth	3.69 (0.44)	2.39 (0.28)	3.26 (0.09)	3.32 (0.41)	2.55 (0.33)	2.23 (0.22)
	p=0.0041		p=0.8376		p=0.2483	
Proliferative zone depth	2.18 (0.38)	1.55 (0.12)	2.20 (0.08)	2.33 (0.17)	1.43 (0.27)	1.19 (0.21)
	p=0.0394		p=0.3233		p=0.2938	
Hypertrophic zone depth	1.36 (0.13)	0.84 (0.23)	0.94 (0.01)	1.08 (0.18)	0.98 (0.17)	1.03 (0.13)
	p=0.0045		p=0.3021		p=0.7083	
Average(SD); **p<0.05**						

Figure 1. Ezh2 inactivation in mesenchymal progenitor, osteoblast, and chondrocyte lineages. *A*, overview of mesenchymal lineage and mouse *Cre* drivers. Lineage-specific conditional inactivation of *Ezh2* using the mesenchymal progenitor driver *Prrx1-Cre*, the osteoprogenitor driver *Osx1*-Cre, and the chondroprogenitor driver *Col2a1-Cre* was performed. *B*, Alcian blue/eosin analysis of proximal tibiae from WT and cKO mice at adolescence. *C*, average depth, growth plate depth, and hypertrophic zone depths within the growth plate were determined using ImageJ software. *D*, comparison of epiphysis and growth plate depth in WT and cKO animals. *, $p < 0.05$; **, $p < 0.01$; ***, $p < 0.001$.

were up-regulated on day 14 (Fig. 4*E*). Gene expression showed strong concordance between RNA-Seq and real-time quantitative PCR (Fig. 4, *E* and *F*).

To further understand the transcriptional effects of *Ezh2* inactivation, we performed differential gene expression analysis (>0.1 RPKM in cKO groups) between WT and cKO IMC cultures at each time point and observed 57 genes that were commonly up-regulated >1.4-fold in cKO compared with WT IMC cultures (Fig. 5*A*). These genes included osteogenic extracellular matrix proteins such as *Ibsp*, *Bglap*, and *Wnt16* as well as *Cyp27b1*, *Ebf2*, and *Otor* (Fig. 5*B*).

Functional gene annotation clustering using DAVID 6.7 (>0.1 RPKM expression of WT or cKO at each time point) shows that, in day 3 IMC cultures, *Ezh2* inactivation led to the enrichment of functional categories, including "signal," "extracellular matrix," and "growth factor" (Table S2). Similar functional categories were also observed on day 7 of culture; however the "bone development" gene cluster was also notably

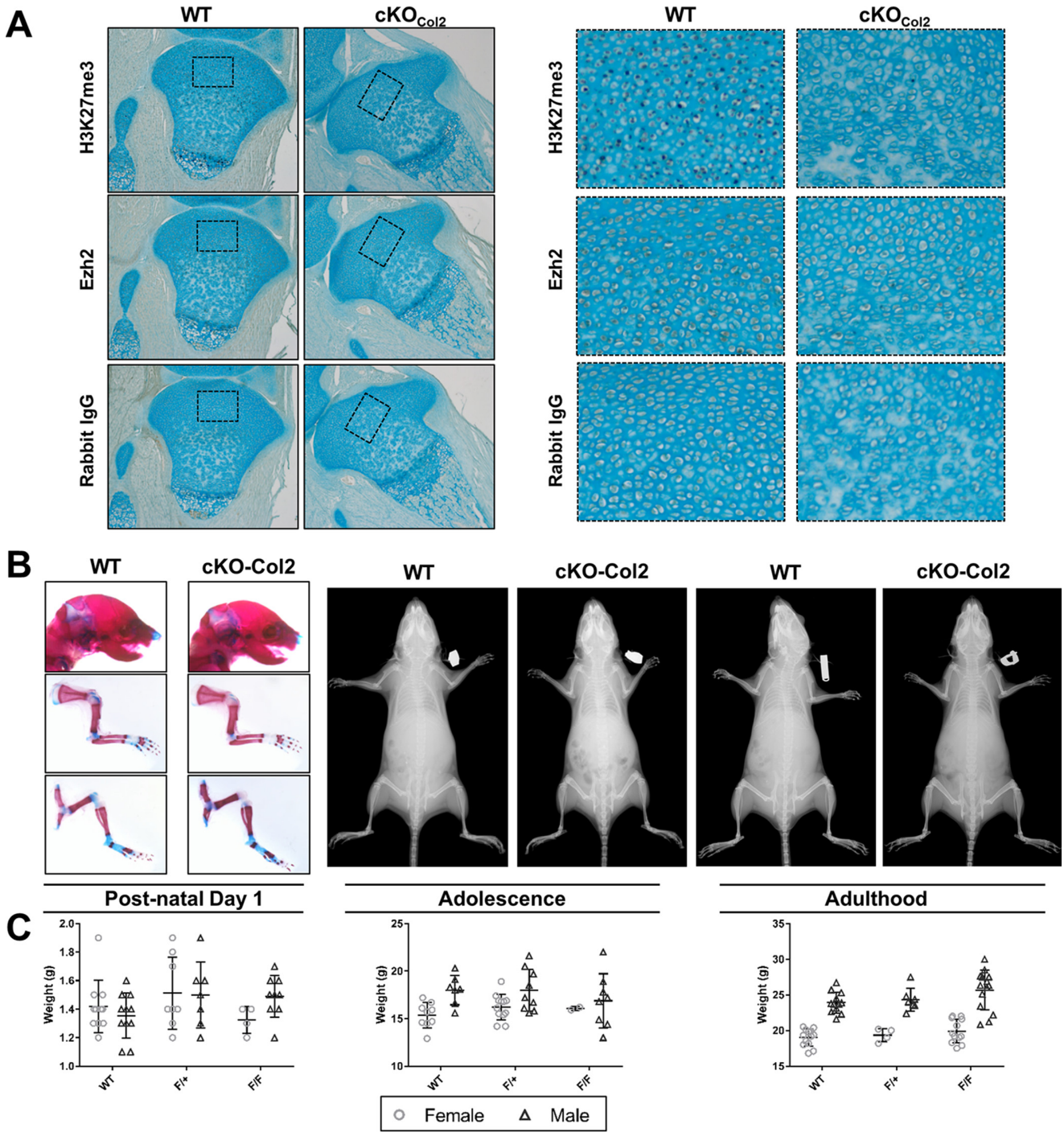

Figure 2. Cartilage-specific deletion of *Ezh2* does not affect skeletal developmental. *A*, immunohistochemical analysis of H3K27me3 and *Ezh2* abundance in proximal tibiae from post-natal day 1 WT and cKO$_{Col2}$ mice. *B*, Alcian blue/alizarin red whole-mount staining did not reveal growth abnormalities in post-natal day 1 mice (*left panels*), and radiographic analysis was similar between WT and cKO$_{Col2}$ mice at 4 weeks (*center panels*) and 8 weeks of age (*right panels*). *C*, body weight was used as an indicator for altered growth. On post-natal day 1, adolescence, and adulthood, the body weights were similar between genotypes.

enriched in cKO IMCs. Furthermore, *Ezh2* inactivation led to the enrichment of a number of osteogenic functional categories on day 14, including "regulation of ossification," "calcium signaling pathway," "skeletal system development," and "bone development" Table S2).

Functional annotation analysis suggests that *Ezh2* inactivation enhances ossification; therefore, we re-evaluated the RNA-Seq results using a curated list of 93 genes that are relevant to skeletal development to determine whether osteogenesis was enhanced in cKO IMCs. Hierarchical clustering of this curated skeletal gene list revealed that day 3 IMC cultures expressed a distinct chondrogenic gene cluster that was down-regulated over time (Fig. 6*A*). Conversely, an osteogenic gene cluster including *Sp7(Osx)*, *Runx2*, *Ibsp*, and *Bglap* was up-regulated in day 14 samples and had the greatest relative expression in cKO IMC cultures (Fig. 6*A*). Several osteogenic genes were

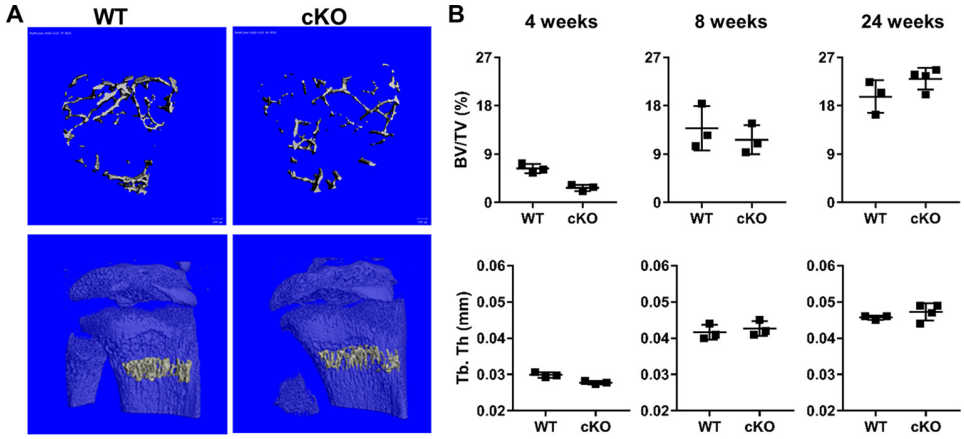

Figure 3. Ezh2-deficient adolescent mice exhibit reduced bone density that is restored during adulthood. *A*, representative micro-CT 3D reconstruction of the proximal tibial metaphysis of WT and cKO_{Col2} mice. *B*, BV/TV and Tb.Th measured in the proximal tibial metaphysis were lower in *Ezh2*-deficient mice at 4 weeks of age ($n = 3$/group), although, upon skeletal maturity (8 weeks), no differences were observed ($n = 3$/group). Further, these parameters were also unchanged at 24 weeks of age when measured in the lumbar vertebrae (WT, $n = 3$; cKO, $n = 4$). *, $p < 0.05$.

expressed at 2-fold higher levels in cKO compared with WT IMC cultures on day 14 (Fig. 6*B*). As an important regulator of osteogenic differentiation, we evaluated whether the transcription factor *Sp7(Osx)* was also up-regulated at the protein level. *Sp7(Osx)* was present at higher levels in cKO IMC cultures compared with the WT on day 7 and furthermore at day 14 (Fig. 6*C*). Together, these data demonstrate that *Col2a1*-specific deletion of *Ezh2* enhances the expression of osteogenic genes within the cartilage tissue.

Ezh2 inactivation does not promote ossification of cartilage in vivo

Because *Ezh2* inactivation lead to enhanced expression of osteogenic factors *in vitro*, we screened 6-month-old WT and cKO mice for early bony changes that are seen in early osteoarthritis. Radiographic analysis of WT and cKO mice did not show evidence of abnormalities consistent with early osteoarthritic change (Fig. 2). In addition, micro-CT analysis of the knee joint of WT and cKO mice did not reveal the presence of osteophytes or irregularities within the subchondral bone that would be expected with bony osteoarthritic change (Fig. 6*D*). These results suggest that Ezh2 loss in *Col2a1*-expressing cells does not promote cartilage mineralization and formation of hypertrophic chondrocytes.

Discussion

The results of this investigation, in which *Ezh2* was knocked down using the *Col2a1* driver, demonstrate that *Ezh2* deficiency leads to a global reduction in H3K27me3 in chondrocytes. This decrease in H3K27me3 does not appear to impact normal skeletal development or impair the protective function of mature articular cartilage compared with *Ezh2* inactivation in mesenchymal progenitor cells. Notably, transcriptome analysis of *in vitro* IMC cultures derived from WT and cKO mice shows that chondrocytes with *Ezh2* knockdown display enhanced osteogenesis. This program is characterized by increased expression of bone-related genes, including the transcription factors *Sp7(Osx)*, extracellular matrix genes, including *Ibsp* and *Bglap*, and signaling factors such as *Bmp2* and *Wnt16*. This study suggests that H3K27me3 mediated by *Ezh2* has only minimal impact and appears to be dispensable for chondrogenic differentiation. Our study also provides evidence for *Ezh2* as an important factor in regulating osteogenic differentiation of chondrocytes.

Ezh2 is critical for early embryonic development (32, 33). However, mice are able to survive to adulthood when *Ezh2* is inactivated in mesenchymal progenitors using the *Prrx1-Cre* driver (2, 4, 30). Although viable, these mice exhibit significant skeletal developmental abnormalities, including short stature and limb segments, premature closure of the cranial sutures, and clinodactyly, findings reminiscent of Weaver syndrome in humans (34). Interestingly, loss of *Ezh2* in osteoblasts results in normal-looking animals that exhibit a low bone mass phenotype (35). Our findings that loss of *Ezh2* activity in the chondrocyte linage does not lead to alterations in skeletal development indicates that previous observations of skeletal abnormalities are the result of *Ezh2* effects on mesenchymal progenitor cells and skeletal patterning (2, 4, 30).

While this study was in progress, Lui *et al.* (36) published a study of the phenotype of mice with dual inactivation of *Ezh1* and *Ezh2* in chondrocytes. The chondrocyte-specific loss of *Ezh2* alone was not specifically reported (36), but the dual knockout mice exhibit significant growth retardation. However, the data presented by Lui *et al.* (36) indicates that *Ezh1* and *Ezh2* may potentially compensate for each other during skeletal development. The skeletal role of Eed, a member of the PRC2 complex that is required for *Ezh1* or *Ezh2* activity, was also recently evaluated (31). Inactivation of this scaffolding protein produced severe skeletal deformities, including kyphosis, short stature, and an increase in hypertrophic chondrocyte differentiation. These changes were similar but distinctly different from the changes observed in the dual *Ezh1*/*Ezh2* knockout mice (36). In the context of our work, these studies indicate that *Ezh1* and *Ezh2* have redundant functionality within chondrocytes and may compensate, at least partially for the loss of each other.

Ezh1 and *Ezh2* have been shown previously to regulate H3K27 methylation and chromatin compaction by different mechanisms (37). Specifically, the histone methyltransferase activity of *Ezh1* was found to be 20-fold weaker compared with

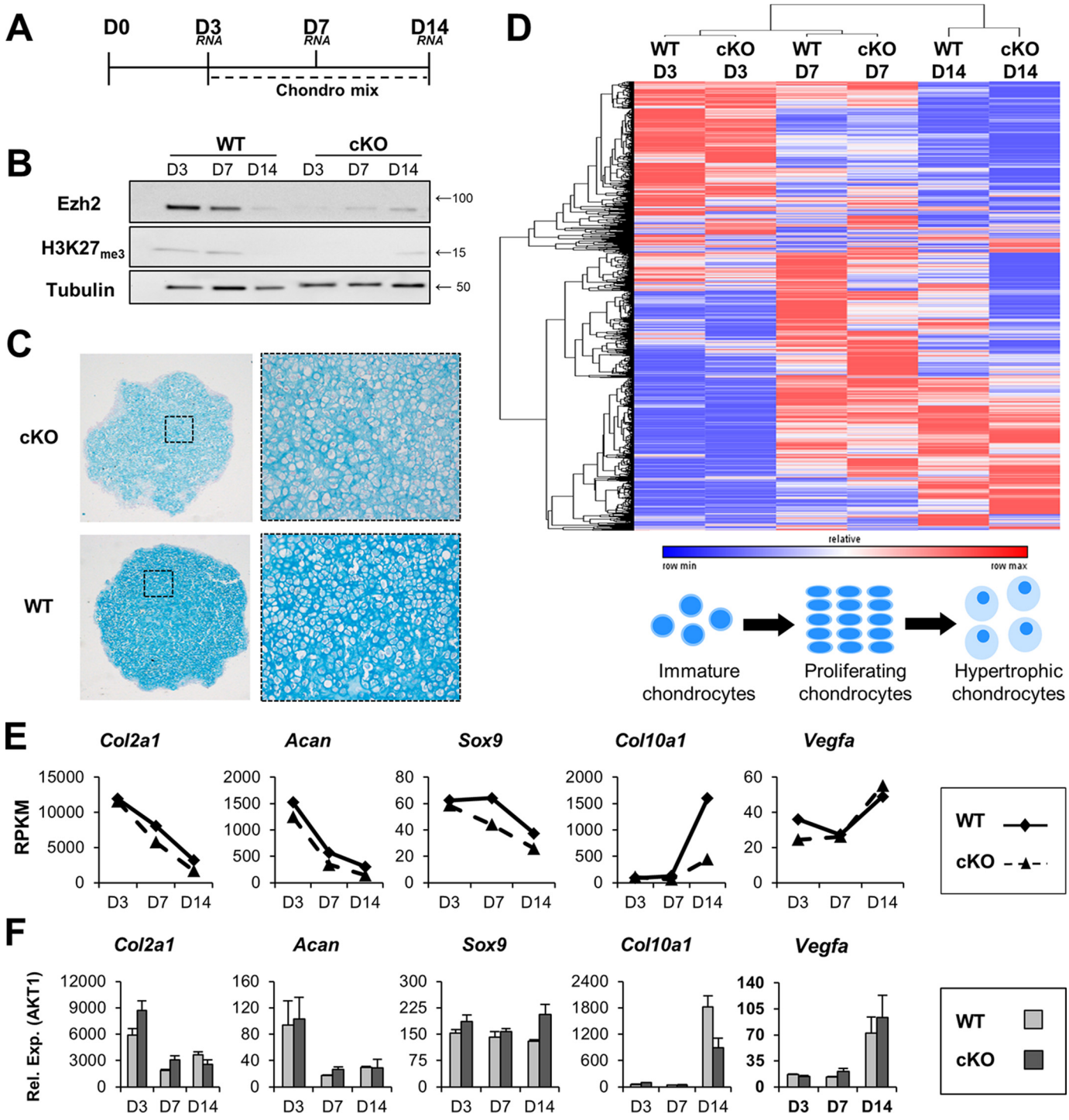

Figure 4. Chondrogenic genes exhibit normal expression upon loss of *Ezh2* and H3K27me3. *A*, IMCs were isolated from WT (*Ezh2*$^{f/f}$; *Col2a1-Cre*$^{-/-}$) and cKO$_{Col2}$ mice and plated in micromass culture for 14 days (*D*) in the presence of chondrogenic mixture (*Chondro mix*). *B*, abundance of *Ezh2* and H3K27me3 was reduced in cKO$_{Col2}$ micromasses compared with the WT. The numbers on the *right* indicate locations of molecular weight markers (kilodalton). *C*, histological staining of WT (*Ezh2*$^{f/f}$; *Col2a1-Cre*$^{-/-}$) and cKO$_{Col2}$ micromasses show a reduced Alcian blue extracellular matrix in cKO$_{Col2}$ chondrocytes. *D*, RNA-Seq analysis was performed on WT (*Ezh2*$^{f/f}$; *Col2a1-Cre*$^{-/-}$) and cKO$_{Col2}$ IMCs on day 3, day 7, and day 14 of culture. Gene expression data were filtered to exclude genes that were not expressed in any of the samples (0 RPKM, 19,641 of 23,359 genes were visualized). Hierarchical clustering of the filtered RNA-Seq identified three clusters that grouped together WT and cKO$_{Col2}$ samples taken at similar time points, indicating that the majority of expressed genes were similar between samples. *E*, chondrogenic genes associated with immature and proliferating chondrocytes (*Col2a1*, *Acan*, and *Sox9*) are highly expressed on day 3, whereas the hypertrophic markers *Col10a1* and *Vegfa* are up-regulated on day 14. *F*, validation of RNA-Seq data shows good concordance with quantitative PCR.

Ezh2. However, *Ezh1* was more potent than *Ezh2* in compacting chromatin independent of histone methylation. Despite mechanistic differences in chromatin regulation, *Ezh1* was shown to regulate a subset of *Ezh2* target genes, reinforcing the idea that these proteins may potentially compensate for each other. In addition to mechanism-related differences, *Ezh1* and *Ezh2* may be expressed at different stages of mesenchymal differentiation (2, 19). Previous studies suggest that *Ezh2* is expressed in pro-

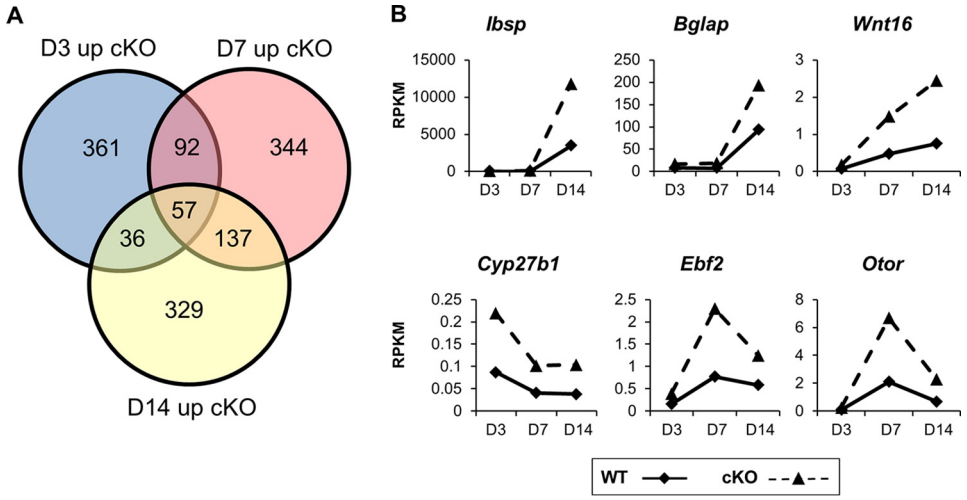

Figure 5. Differential gene expression analysis shows up-regulation of osteogenic genes in *Ezh2*-deficient immature chondrocyte cultures. *A*, differential gene expression analysis of RNA-Seq from WT (*Ezh2*$^{wt/wt}$; *Col2a1-Cre*$^{+/-}$) and cKO$_{Col2}$ immature chondrocytes revealed 57 genes that were commonly up-regulated more than 1.4-fold in *Ezh2*-deficient cultures on days 3, 7, and 14. The analysis was limited to genes with a minimal expression of 0.1 RPKM in the cKO group at each time point. *B*, the osteogenic extracellular matrix genes *Ibsp*, *Bglap*, and *Wnt16* were up-regulated in cKO$_{Col2}$ chondrocytes as well as some nonosteogenic genes such as *Cyp27b1*, *Ebf2*, and *Otor*.

liferating uncommitted mesenchymal stem cells, whereas *Ezh1* may be more important for post-proliferative lineage-committed cells. Although these proteins are partially redundant, it appears that *Ezh1* and *Ezh2* differ in spatio-temporal expression and may have different mechanistic activities during mesenchymal differentiation and skeletal development.

In this study, *in vivo* immunohistochemical staining resulted in a modest reduction of *Ezh2* protein but a more robust depletion of its enzymatic target H3K27me3. It is possible that chondrocytes that express one or both copies of the *Ezh2* WT allele have a selective growth advantage. The discrepancy between modest *Ezh2* loss and more robust H3K27me3 loss suggests that the residual *Ezh2* protein may lack enzymatic activity. Indeed, we have shown recently that recombinase activity with this *Ezh2* conditional model results in the production of the truncated mRNA and protein (35). In this study, we also provide evidence indicating that the truncated *Ezh2* mRNA is detectable after recombination. Thus, although *Ezh2* protein is detected by immunohistochemical staining *in vivo*, it is anticipated that a portion of this protein lacks enzymatic activity. Thus, the cumulative effects of *Ezh2* protein loss and the presence of the enzymatically inactive *Ezh2* may account for a significant loss of H3K27me3 within chondrocytes.

In our study, modification of *Ezh2*'s enzymatic function through genetic inactivation resulted in reduced H3K27me3 in chondrocytes, but the expression of chondrogenic genes was unchanged. A previous study utilizing the *Ezh2* inhibitor UNC1999 to treat chondrocytes *in vitro* observed a slight reduction in hypertrophic cell size and decreased expression of the hypertrophic markers *Col10a1* and *Ihh* (36). We also observed reduced *Col10a1* and *Ihh* (data not shown) in IMC cultures, although the impact of these changes *in vivo* appears to be minimal. Conversely, global knockout of the H3K27me3 demethylase *Jmjd3*(*Kdm6b*) severely impaired the proliferation and differentiation of chondrocytes, resulting in reduced endochondral ossification (27). Collectively, these data suggest that *Ezh2* is dispensable for chondrocyte differentiation, including early hypertrophic differentiation during endochondral ossification.

Chondrocytes deficient in *Ezh2* exhibit enhanced expression of osteogenic genes in vitro, including *Bmp2*, *Ibsp*, *Sp7(Osx)*, and others. Our results support previous observations in which siRNA or pharmacological inactivation of *Ezh2* accelerates osteogenic differentiation of human mesenchymal stromal cells and mouse preosteoblast cells (2, 3, 22, 31, 38, 39). Furthermore, a pharmacological inhibitor of *Ezh2 in vivo* was also found to prevent bone loss in estrogen deficiency models (3, 39, 40). Although Fang *et al.* (40) have proposed that loss of *Ezh2* activity leads to inhibition of osteoclastogenesis, our results also support a direct bone anabolic mechanism for *Ezh2* inhibition (3). Thus, *Ezh2* inhibitors may be effective therapeutic agents for osteoporosis treatment via dual mechanisms: enhancement of bone anabolic activity and inhibition of bone resorption.

Even though enhanced osteogenic potential of chondrocytes was observed *in vitro* in this study, this biological effect did not result in early-onset osteoarthritis in *Ezh2* KO mice. Consistent with these findings, Chen *et al.* (41) observed that *EZH2* expression is increased in human osteoarthritis and up-regulated in response to inflammation (interleukin 1β). In addition, they also evaluated the *Ezh2* inhibitor EPZ005687 as a therapeutic agent for treating cartilage degeneration and observed delayed osteoarthritis development *in vivo*. These results are encouraging and warrant further investigation of the specific role of *Ezh2* in the development of osteoarthritis (41).

In summary, *Ezh2* regulates H3K27me3 in chondrocytes, and its cartilage-specific inactivation does not lead to skeletal defects observed in early mesenchymal progenitors. Furthermore, *Ezh2* deficiency does not modulate the expression of chondrogenic genes *in vitro*. However, in both the chondrogenic and osteogenic lineages, we found that *Ezh2* inactivation promotes an osteogenic gene expression program. Thus, *Ezh2* may normally function to suppress the bone phenotype in distinct mesenchymal lineages.

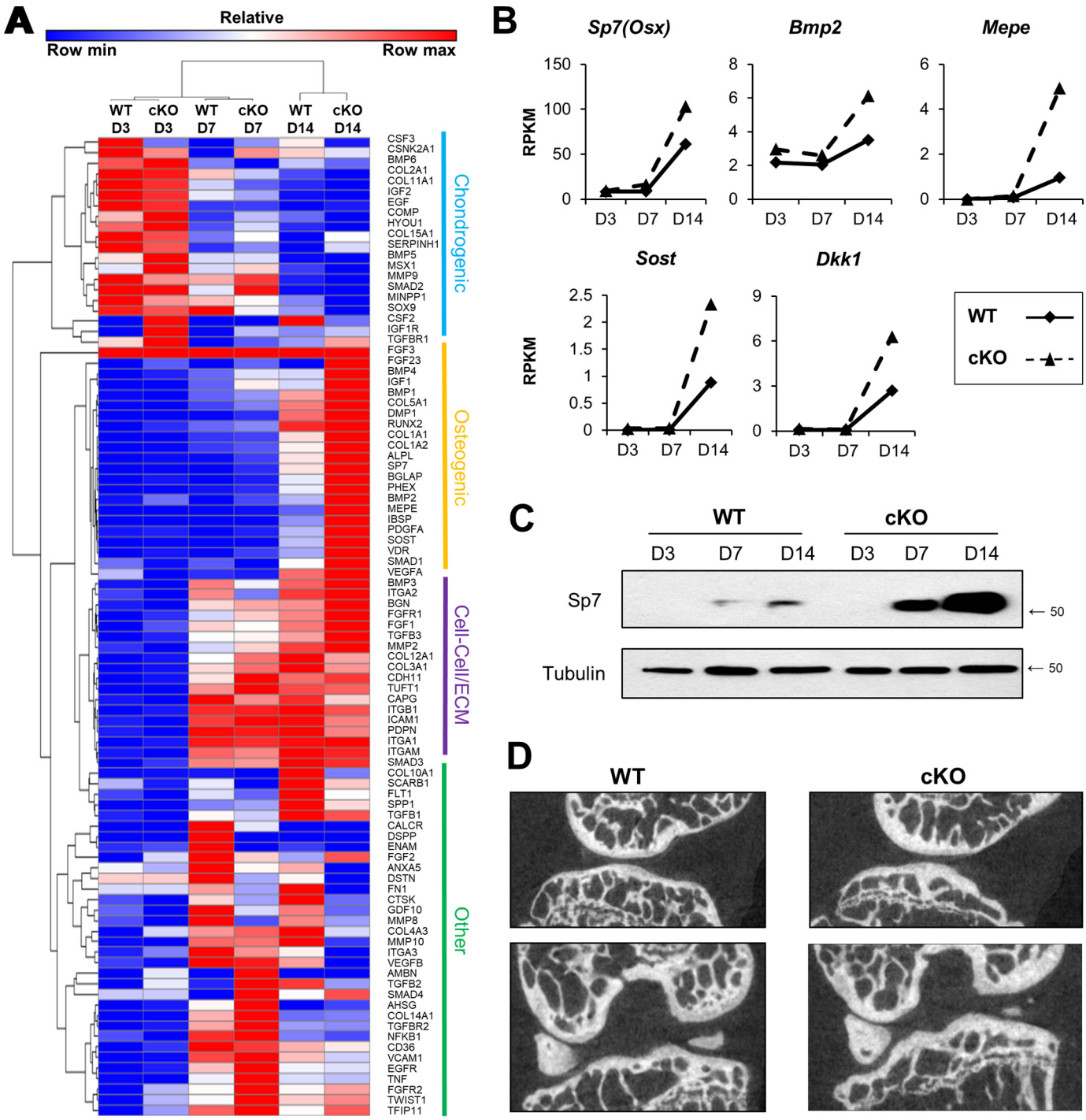

Figure 6. Ezh2-deficient chondrocytes exhibit enhanced expression of an osteogenic-program *in vitro*, but genetic inactivation does not result in osteoarthritis *in vivo*. *A*, expression of chondrogenic, osteogenic, cell–cell contact/extracellular matrix, and other genes by RNA-Seq. *Ezh2*-deficient IMCs exhibit up-regulation of osteogenic genes on day 14 compared with WT (*Ezh2*$^{wt/wt}$; *Col2a1-Cre*$^{+/-}$) IMC cultures. *B*, osteoblast-associated genes, including *Sp7(Osx)* and *Bmp2*, the osteocyte-associated extracellular matrix gene *Mepe*, as well as the WNT pathway inhibitors *Sost* and *Dkk1* are up-regulated in cKO$_{Col2}$ IMC cultures. *C*, protein levels of the transcription factor *Sp7(Osx)* were also enhanced in *Ezh2*-deficient IMC cultures. The numbers on the *right* indicate the location of molecular weight markers (kilodalton). *D*, WT and cKO$_{Col2}$ mice were aged to 24 weeks, and micro-CT analysis was performed on the right knee joint. No changes in the subchondral bone were observed (n = 4/group).

Experimental procedures

Ezh2-deficient mice

The Mayo Clinic Institutional Animal Care and Use Committee preapproved all animal experimentation, and studies were conducted according to guidelines provided by the National Institutes of Health and the Institute of Laboratory Animal Resources, National Research Council. Mice harboring two copies of the *Ezh2* allele with *loxP* sites flanking the SET domain (*Ezh2*$^{fl/fl}$) were obtained from the Mutant Mouse Regional Resource Centre (B6;129P2-*Ezh2*tm1Tara/Mmnc, University of North Carolina, Chapel Hill, NC). Homozygous animals (*Ezh2*$^{fl/fl}$) were crossed with *Col2a1-Cre* (21, 42),

Prrx1-Cre (2, 43), or *Osx1-Cre* (44) mice to inactivate *Ezh2* function in, respectively, developing chondrocytes, mesenchymal progenitor cells, or osteoprogenitor cells. Animals were housed in an accredited facility under a 12-h light/dark cycle and provided water and food (PicoLab Rodent Diet 20, LabDiet) *ad libitum*. These crosses generated WT (WT, $Ezh2^{wt/wt}$: *Col2a1-Cre*+; WT, $Ezh2^{wt/wt}$: *Prrx1-Cre*+; WT, $Ezh2^{wt/wt}$: *Osx1-Cre*+), $Ezh2^{fl/fl}$: $Col2a1\text{-}Cre^{-/-}$, and conditional knockout (cKO-Col2, $Ezh2^{fl/fl}$: Col2a1-*Cre*+; cKO-Prrx1, $Ezh2^{fl/fl}$: Prrx1-*Cre*+; cKO-Osx, $Ezh2^{fl/fl}$; Osx1-Cre+) animals. The following primers were used for genotyping: *Ezh2*, TGTCATGTCTGGGTCTAATGCTAC (forward) and GGAACCTCGCTATGTGTAACCA (reverse); Col2a1-*Cre*, CCAATTTACTGACCGTACACCAA (forward) and CCTGATCCTGGCAATTTCGGCTA (reverse). *Prrx1-Cre* and *Osx1-Cre* mice were genotyped as described previously (2, 21).

Isolation and culture of immature mouse chondrocytes

Primary IMCs were isolated from post-natal day 5 mice as described previously by Gosset *et al.* (45). Freshly isolated IMCs were resuspended at a concentration of 2×10^7 cells/ml in growth medium (Dulbecco's modified Eagle's medium with 2% fetal bovine serum and 1% anti-mycotic/antibiotic) and plated in micromass culture by pipetting 10 μl of cell suspension onto a low-adhesion tissue culture dish with up to 3 micromasses/dish. Micromasses formed by incubation for 1 h at 37 °C and 5% CO_2, after which growth medium was carefully added and left undisturbed for 3 days. Following micromass formation, the growth medium was replaced with differentiation medium (growth medium with 1× insulin–transferrin–selenium solution (Life Technologies), 0.05 mg/ml ascorbic acid, and 10 mM β-glycerol phosphate) on day 3 of culture, and the differentiation medium was replaced every 3–4 days.

Radiographic and micro-CT analysis

Radiographic analysis was performed using a Faxitron X-ray imaging cabinet (Faxitron Bioptics, Tucson, AZ). Quantitative analysis of the spine was performed using a vivaCT 40 scanner (SCANCO Medical AG) with the following parameters: $E = 55$ kVp, $I = 145$ μA, integration time = 300 ms (where E = energy, kVp = kilovoltage peak, and I = intensity). A 10.5-μm voxel size using a threshold of 220 was applied to all scans at high resolution. Two-dimensional data from scanned slices were used for 3D analysis of morphometric parameters of trabecular bone mass and microarchitecture, including BV/TV, Tb.N, Tb.Th, Tb.Sp, and the structure model index (SMI), an indicator of plate-like *versus* rod-like trabecular architecture.

Morphological and histology analysis

Whole-mount staining of skeletal preparations was performed as described previously (2). For histological analyses, mice were sacrificed either on post-natal day 1, 3, 4, or 8 or at 24 weeks of age, and the right hind limb was fixed in 10% neutral buffered formalin, decalcified with 15% EDTA, and embedded in paraffin. Micromass cultures were also fixed with 10% neutral buffered formalin before dehydration and paraffin embedding. Serial sections were taken at 5-μm thickness and stained with hematoxylin and eosin, Alcian blue/eosin, or Safranin O/fast green/hematoxylin.

Immunohistochemical staining

The right hind limbs or tibiae from mice on post-natal day 1, 4, or 8 or from 24-week-old mice were prepared as described above. IHC was performed on serial sections of 5-μm thickness using the Mouse- and Rabbit-Specific HRP (ABC) Detection IHC Kit (Abcam) and the DAB Enhanced Liquid Substrate System (Sigma-Aldrich) according to the instruction manuals. The primary antibodies used were Ezh2 (1:50, 07-689, Millipore), H3K27me3 (1:150, 17-622, Millipore), and rabbit isotype control (rabbit IgG, 1:50, AB-150-C, R&D Systems). Slides were counterstained with Alcian blue.

RNA isolation, reverse transcription, and real-time quantitative PCR

IMC cultures were harvested on days 3, 7, and 14 for RNA analysis. Briefly, micromasses were washed with PBS to remove medium and mechanically disrupted with a scalpel, and then 700 μl of QIAzol was added to lyse cells. Total RNA was extracted using the miRNeasy MicroKit (Qiagen), and 1 μg of RNA was used as template for reverse transcription reactions. The Superscript III First Strand Synthesis System (Life Technologies) was used to convert RNA to complementary DNA. Real-time PCR reactions were composed of 10 ng of complementary DNA, gene-specific primers (Table S3), and 1× QuantiTect SYBR® Green PCR Master Mix (Qiagen) with a final volume of 10 μl and detected using the CFX384 real time system machine (Bio-Rad). Relative transcript abundance of genes of interest was normalized to AKT1 expression using the $2^{-\Delta\Delta Ct}$ method.

Western blotting

Total protein was harvested from IMC cultures on days 3, 7, and 14 of culture. Micromasses were washed with PBS, mechanically disrupted with a scalpel in the presence of radioimmunoprecipitation buffer (150 mM NaCl, 50 mM Tris (pH 7.4), 1% w/v sodium deoxycholate, 0.1% w/v SDS, and 1% v/v Triton X-100) supplemented with protease inhibitor mixture (Sigma) and phenylmethylsulfonyl fluoride (Sigma) and stored at −80 °C until quantification. Protein content was quantified using the DC™ protein assay (Bio-Rad) according to the manufacturer's protocol. Western blotting and membrane development were performed as described previously (2), and the following primary antibodies were used to detect proteins: Ezh2 (1:10,000, 5848, Cell Signaling Technology), H3K27me3 (1:5000, 17-622, Millipore), SP7 (1:1000, ab22552, Abcam), and tubulin (1:10,000, E7, Developmental Studies Hybridoma Bank (DSHB), University of Iowa).

RNA-Seq and bioinformatics analysis

Whole-transcriptome sequencing and bioinformatics analyses were performed as described previously (46). The TruSeq RNA sample Prep Kit v2 (Illumina) was used to prepare RNA samples, and then samples were analyzed using the Illumina HiSeq 2000 with the TruSeq SBS sequencing kit version 3 and HCS v2.0.12 data collection software. Following data collection,

sequence data were processed using MAPRSeq (v.1.2.1) and the bioinformatics workflow (TopHat 2.0.6, HTSeq, and edgeR 2.6.2), where expression data were normalized using the reads per kilobase per million (RPKM) method.

Hierarchical clustering was performed using GENE-E (version 3.0.228, Broad Institute, Cambridge, MA), and DAVID Bioinformatics Resources 6.7 (http://david.abcc.ncifcrf.gov) was used to perform gene functional annotation analysis (47, 49).

Image quantitation

Images were digitally photographed using the AxioVert A1 (Zeiss) and Zen software packages (Zeiss). Growth plate depth was evaluated using National Institutes of Health ImageJ software (48).

Statistical analysis

Data obtained are presented as the mean ± S.D. Statistical analysis was performed using JMP® Pro v10.0.0 (SAS Institute), and p values were determined with the nonparametric Wilcoxon test. Significance is noted in the figures when applicable (*, $p < 0.05$; **, $p < 0.01$; ***, $p < 0.001$).

Author contributions—E. C., A. D., S. M. R., C. G.-G., and A. J. v. W. conceptualization; E. C., A. D., S. M. R., C. G.-G., C. R. P., E. W. B., M. E. M.-L., and H.-J. I. data curation; E. C., A. D., J. J. W., and A. N. L. formal analysis; E. C., M. K., A. J. K., J. J. W., A. N. L., and A. J. v. W. supervision; E. C., A. D., S. M. R., and A. J. v. W. funding acquisition; E. C. and A. D. investigation; E. C., A. D., S. M. R., C. G.-G., C. R. P., E. W. B., M. E. M.-L., H.-J. I., M. K., A. J. K., and J. J. W. methodology; E. C., A. D., S. M. R., C. G.-G., and A. J. v. W. writing-original draft; E. C. and A. J. v. W. project administration; E. C., A. D., S. M. R., C. G.-G., C. R. P., E. W. B., M. E. M.-L., H.-J. I., M. K., A. J. K., J. J. W., A. N. L., and A. J. v. W. writing-review and editing.

Acknowledgments—We thank Oksana Pichurin, David Razidlo, Bridget Stensgard, and Bashar Hassan for technical support and the members of our laboratories for stimulating discussions. We also acknowledge support from the Bioinformatics Core, Medical Genome Facility, and Robert and Arlene Kogod Center on Aging at the Mayo Clinic.

References

1. Arrowsmith, C. H., Bountra, C., Fish, P. V., Lee, K., and Schapira, M. (2012) Epigenetic protein families: a new frontier for drug discovery. *Nat. Rev. Drug Discov.* **11,** 384–400 CrossRef Medline
2. Dudakovic, A., Camilleri, E. T., Xu, F., Riester, S. M., McGee-Lawrence, M. E., Bradley, E. W., Paradise, C. R., Lewallen, E. A., Thaler, R., Deyle, D. R., Larson, A. N., Lewallen, D. G., Dietz, A. B., Stein, G. S., Montecino, M. A., *et al.* (2015) Epigenetic Control of Skeletal Development by the Histone Methyltransferase Ezh2. *J. Biol. Chem.* **290,** 27604–27617 CrossRef Medline
3. Camilleri, E. T., Gustafson, M. P., Dudakovic, A., Riester, S. M., Garces, C. G., Paradise, C. R., Takai, H., Karperien, M., Cool, S., Sampen, H. J., Larson, A. N., Qu, W., Smith, J., Dietz, A. B., and van Wijnen, A. J. (2016) Identification and validation of multiple cell surface markers of clinical-grade adipose-derived mesenchymal stromal cells as novel release criteria for good manufacturing practice-compliant production. *Stem Cell Res. Ther.* **7,** 107 CrossRef Medline
4. Hemming, S., Cakouros, D., Codrington, J., Vandyke, K., Arthur, A., Zannettino, A., and Gronthos, S. (2017) EZH2 deletion in early mesenchyme compromises postnatal bone microarchitecture and structural integrity and accelerates remodeling. *FASEB J.* **31,** 1011–1027 CrossRef Medline
5. Carpio, L. R., Bradley, E. W., McGee-Lawrence, M. E., Weivoda, M. M., Poston, D. D., Dudakovic, A., Xu, M., Tchkonia, T., Kirkland, J. L., van Wijnen, A. J., Oursler, M. J., and Westendorf, J. J. (2016) Histone deacetylase 3 supports endochondral bone formation by controlling cytokine signaling and matrix remodeling. *Sci. Signal.* **9,** ra79 CrossRef Medline
6. Goldring, M. B., and Marcu, K. B. (2012) Epigenomic and microRNA-mediated regulation in cartilage development, homeostasis, and osteoarthritis. *Trends Mol. Med.* **18,** 109–118 CrossRef Medline
7. Barter, M. J., Bui, C., and Young, D. A. (2012) Epigenetic mechanisms in cartilage and osteoarthritis: DNA methylation, histone modifications and microRNAs. *Osteoarthritis Cartilage* **20,** 339–349 CrossRef Medline
8. Bradley, E. W., Carpio, L. R., van Wijnen, A. J., McGee-Lawrence, M. E., and Westendorf, J. J. (2015) Histone deacetylases in bone development and skeletal disorders. *Physiol. Rev.* **95,** 1359–1381 CrossRef Medline
9. Gordon, J. A. R., Stein, J. L., Westendorf, J. J., and van Wijnen, A. J. (2015) Chromatin modifiers and histone modifications in bone formation, regeneration, and therapeutic intervention for bone-related disease. *Bone* **81,** 739–745 CrossRef Medline
10. Schwarz, D., Varum, S., Zemke, M., Schöler, A., Baggiolini, A., Draganova, K., Koseki, H., Schübeler, D., and Sommer, L. (2014) Ezh2 is required for neural crest-derived cartilage and bone formation. *Development* **141,** 867–877 CrossRef Medline
11. Pike, J. W., Meyer, M. B., St John, H. C., and Benkusky, N. A. (2015) Epigenetic histone modifications and master regulators as determinants of context dependent nuclear receptor activity in bone cells. *Bone* **81,** 757–764 CrossRef Medline
12. Meyer, M. B., Benkusky, N. A., Sen, B., Rubin, J., and Pike, J. W. (2016) Epigenetic plasticity drives adipogenic and osteogenic differentiation of marrow-derived mesenchymal stem cells. *J. Biol. Chem.* **291,** 17829–17847 CrossRef Medline
13. Wu, H., Gordon, J. A., Whitfield, T. W., Tai, P. W., van Wijnen, A. J., Stein, J. L., Stein, G. S., and Lian, J. B. (2017) Chromatin dynamics regulate mesenchymal stem cell lineage specification and differentiation to osteogenesis. *Biochim. Biophys. Acta* **1860,** 438–449 CrossRef Medline
14. Riester, S. M., Denbeigh, J. M., Lin, Y., Jones, D. L., de Mooij, T., Lewallen, E. A., Nie, H., Paradise, C. R., Radel, D. J., Dudakovic, A., Camilleri, E. T., Larson, D. R., Qu, W., Krych, A. J., Frick, M. A., *et al.* (2017) Safety studies for use of adipose tissue-derived mesenchymal stromal/stem cells in a rabbit model for osteoarthritis to support a phase I clinical trial. *Stem Cells Transl. Med.* **6,** 910–922 CrossRef Medline
15. Caplan, A. I. (2016) MSCs: The sentinel and safe-guards of injury. *J. Cell. Physiol.* **231,** 1413–1416 CrossRef Medline
16. Deng, Z. L., Sharff, K. A., Tang, N., Song, W. X., Luo, J., Luo, X., Chen, J., Bennett, E., Reid, R., Manning, D., Xue, A., Montag, A. G., Luu, H. H., Haydon, R. C., and He, T. C. (2008) Regulation of osteogenic differentiation during skeletal development. *Front. Biosci.* **13,** 2001–2021 CrossRef Medline
17. Dudakovic, A., Camilleri, E. T., Lewallen, E. A., McGee-Lawrence, M. E., Riester, S. M., Kakar, S., Montecino, M., Stein, G. S., Ryoo, H. M., Dietz, A. B., Westendorf, J. J., and van Wijnen, A. J. (2015) Histone deacetylase inhibition destabilizes the multi-potent state of uncommitted adipose-derived mesenchymal stromal cells. *J. Cell. Physiol.* **230,** 52–62 CrossRef Medline
18. Dudakovic, A., Evans, J. M., Li, Y., Middha, S., McGee-Lawrence, M. E., van Wijnen, A. J., and Westendorf, J. J. (2013) Histone deacetylase inhibition promotes osteoblast maturation by altering the histone H4 epigenome and reduces Akt phosphorylation. *J. Biol. Chem.* **288,** 28783–28791 CrossRef Medline
19. Dudakovic, A., Gluscevic, M., Paradise, C. R., Dudakovic, H., Khani, F., Thaler, R., Ahmed, F. S., Li, X., Dietz, A. B., Stein, G. S., Montecino, M. A., Deyle, D. R., Westendorf, J. J., and van Wijnen, A. J. (2017) Profiling of human epigenetic regulators using a semi-automated real-time qPCR platform validated by next generation sequencing. *Gene* **609,** 28–37 CrossRef Medline
20. Khani, F., Thaler, R., Paradise, C. R., Deyle, D. R., Kruijthof-de Julio, M., Galindo, M., Gordon, J. A., Stein, G. S., Dudakovic, A., and van Wijnen,

A. J. (2017) Histone H4 methyltransferase Suv420h2 maintains fidelity of osteoblast differentiation. *J. Cell. Biochem.* **118,** 1262–1272 CrossRef Medline
21. Bradley, E. W., Carpio, L. R., Olson, E. N., and Westendorf, J. J. (2015) Histone deacetylase 7 (Hdac7) suppresses chondrocyte proliferation and β-catenin activity during endochondral ossification. *J. Biol. Chem.* **290,** 118–126 CrossRef Medline
22. Hemming, S., Cakouros, D., Isenmann, S., Cooper, L., Menicanin, D., Zannettino, A., and Gronthos, S. (2014) EZH2 and KDM6A act as an epigenetic switch to regulate mesenchymal stem cell lineage specification. *Stem Cells* **32,** 802–815 CrossRef Medline
23. Spaapen, F., van den Akker, G. G., Caron, M. M., Prickaerts, P., Rofel, C., Dahlmans, V. E., Surtel, D. A., Paulis, Y., Schweizer, F., Welting, T. J., Eijssen, L. M., and Voncken, J. W. (2013) The immediate early gene product EGR1 and polycomb group proteins interact in epigenetic programming during chondrogenesis. *PLoS ONE* **8,** e58083 CrossRef Medline
24. Wang, H., Meng, Y., Cui, Q., Qin, F., Yang, H., Chen, Y., Cheng, Y., Shi, J., and Guo, Y. (2016) MiR-101 targets the EZH2/Wnt/β-catenin pathway to promote the osteogenic differentiation of human bone marrow-derived mesenchymal stem cells. *Sci. Rep.* **6,** 36988 CrossRef Medline
25. Bradley, E. W., Carpio, L. R., and Westendorf, J. J. (2013) Histone deacetylase 3 suppression increases PH domain and leucine-rich repeat phosphatase (Phlpp)1 expression in chondrocytes to suppress Akt signaling and matrix secretion. *J. Biol. Chem.* **288,** 9572–9582 CrossRef Medline
26. Nakatani, T., Chen, T., and Partridge, N. C. (2016) MMP-13 is one of the critical mediators of the effect of HDAC4 deletion on the skeleton. *Bone* **90,** 142–151 CrossRef Medline
27. Zhang, F., Xu, L., Xu, L., Xu, Q., Li, D., Yang, Y., Karsenty, G., and Chen, C. D. (2015) JMJD3 promotes chondrocyte proliferation and hypertrophy during endochondral bone formation in mice. *J. Mol. Cell. Biol.* **7,** 23–34 CrossRef Medline
28. Ideno, H., Shimada, A., Imaizumi, K., Kimura, H., Abe, M., Nakashima, K., and Nifuji, A. (2013) Predominant expression of H3K9 methyltransferases in prehypertrophic and hypertrophic chondrocytes during mouse growth plate cartilage development. *Gene Expr. Patterns* **13,** 84–90 CrossRef Medline
29. Lawson, K. A., Teteak, C. J., Zou, J., Hacquebord, J., Ghatan, A., Zielinska-Kwiatkowska, A., Fernandes, R. J., Chansky, H. A., and Yang, L. (2013) Mesenchyme-specific knockout of ESET histone methyltransferase causes ectopic hypertrophy and terminal differentiation of articular chondrocytes. *J. Biol. Chem.* **288,** 32119–32125 CrossRef Medline
30. Wyngaarden, L. A., Delgado-Olguin, P., Su, I. H., Bruneau, B. G., and Hopyan, S. (2011) Ezh2 regulates anteroposterior axis specification and proximodistal axis elongation in the developing limb. *Development* **138,** 3759–3767 CrossRef Medline
31. Mirzamohammadi, F., Papaioannou, G., Inloes, J. B., Rankin, E. B., Xie, H., Schipani, E., Orkin, S. H., and Kobayashi, T. (2016) Polycomb repressive complex 2 regulates skeletal growth by suppressing Wnt and TGF-β signalling. *Nat. Commun.* **7,** 12047 CrossRef Medline
32. Müller, J., Hart, C. M., Francis, N. J., Vargas, M. L., Sengupta, A., Wild, B., Miller, E. L., O'Connor, M. B., Kingston, R. E., and Simon, J. A. (2002) Histone methyltransferase activity of a *Drosophila* Polycomb group repressor complex. *Cell* **111,** 197–208 CrossRef Medline
33. O'Carroll, D., Erhardt, S., Pagani, M., Barton, S. C., Surani, M. A., and Jenuwein, T. (2001) The polycomb-group gene Ezh2 is required for early mouse development. *Mol. Cell. Biol.* **21,** 4330–4336 CrossRef Medline
34. Cohen, A. S., Yap, D. B., Lewis, M. E., Chijiwa, C., Ramos-Arroyo, M. A., Tkachenko, N., Milano, V., Fradin, M., McKinnon, M. L., Townsend, K. N., Xu, J., Van Allen, M. I., Ross, C. J., Dobyns, W. B., Weaver, D. D., and Gibson, W. T. (2016) Weaver syndrome-associated EZH2 protein variants show impaired histone methyltransferase function *in vitro*. *Hum. Mutat.* **37,** 301–307 CrossRef Medline
35. Dudakovic, A., Camilleri, E. T., Paradise, C. R., Samsonraj, R. M., Gluscevic, M., Paggi, C. A., Begun, D. L., Khani, F., Pichurin, O., Ahmed, F. S., Elsayed, R., Elsalanty, M., McGee-Lawrence, M. E., Karperien, M., Riester, S. M., *et al.* (2018) Enhancer of zeste homolog 2 (Ezh2) controls bone formation and cell cycle progression during osteogenesis in mice. *J. Biol. Chem.* **293,** 12894–12907 CrossRef Medline
36. Lui, J. C., Garrison, P., Nguyen, Q., Ad, M., Keembiyehetty, C., Chen, W., Jee, Y. H., Landman, E., Nilsson, O., Barnes, K. M., and Baron, J. (2016) EZH1 and EZH2 promote skeletal growth by repressing inhibitors of chondrocyte proliferation and hypertrophy. *Nat. Commun.* **7,** 13685 CrossRef Medline
37. Margueron, R., Li, G., Sarma, K., Blais, A., Zavadil, J., Woodcock, C. L., Dynlacht, B. D., and Reinberg, D. (2008) Ezh1 and Ezh2 maintain repressive chromatin through different mechanisms. *Mol. Cell* **32,** 503–518 CrossRef Medline
38. Hemming, S., Cakouros, D., Vandyke, K., Davis, M. J., Zannettino, A. C., and Gronthos, S. (2016) Identification of novel EZH2 targets regulating osteogenic differentiation in mesenchymal stem cells. *Stem Cells Dev.* **25,** 909–921 CrossRef Medline
39. Jing, H., Liao, L., An, Y., Su, X., Liu, S., Shuai, Y., Zhang, X., and Jin, Y. (2016) Suppression of EZH2 prevents the shift of osteoporotic MSC fate to adipocyte and enhances bone formation during osteoporosis. *Mol. Ther.* **24,** 217–229 CrossRef Medline
40. Fang, C., Qiao, Y., Mun, S. H., Lee, M. J., Murata, K., Bae, S., Zhao, B., Park-Min, K. H., and Ivashkiv, L. B. (2016) Cutting edge: EZH2 promotes osteoclastogenesis by epigenetic silencing of the negative regulator IRF8. *J. Immunol.* **196,** 4452–4456 CrossRef Medline
41. Chen, L., Wu, Y., Wu, Y., Wang, Y., Sun, L., and Li, F. (2016) The inhibition of EZH2 ameliorates osteoarthritis development through the Wnt/β-catenin pathway. *Sci. Rep.* **6,** 29176 CrossRef Medline
42. Ovchinnikov, D. A., Deng, J. M., Ogunrinu, G., and Behringer, R. R. (2000) Col2a1-directed expression of Cre recombinase in differentiating chondrocytes in transgenic mice. *Genesis* **26,** 145–146 CrossRef Medline
43. Logan, M., Martin, J. F., Nagy, A., Lobe, C., Olson, E. N., and Tabin, C. J. (2002) Expression of Cre recombinase in the developing mouse limb bud driven by a Prxl enhancer. *Genesis* **33,** 77–80 CrossRef Medline
44. Rodda, S. J., and McMahon, A. P. (2006) Distinct roles for Hedgehog and canonical Wnt signaling in specification, differentiation and maintenance of osteoblast progenitors. *Development* **133,** 3231–3244 CrossRef Medline
45. Gosset, M., Berenbaum, F., Thirion, S., and Jacques, C. (2008) Primary culture and phenotyping of murine chondrocytes. *Nat. Protoc.* **3,** 1253–1260 CrossRef Medline
46. Dudakovic, A., Camilleri, E., Riester, S. M., Lewallen, E. A., Kvasha, S., Chen, X., Radel, D. J., Anderson, J. M., Nair, A. A., Evans, J. M., Krych, A. J., Smith, J., Deyle, D. R., Stein, J. L., Stein, G. S., *et al.* (2014) High-resolution molecular validation of self-renewal and spontaneous differentiation in clinical-grade adipose-tissue derived human mesenchymal stem cells. *J. Cell. Biochem.* **115,** 1816–1828 CrossRef Medline
47. Huang da, W., Sherman, B. T., and Lempicki, R. A. (2009) Systematic and integrative analysis of large gene lists using DAVID bioinformatics resources. *Nat. Protoc.* **4,** 44–57 CrossRef Medline
48. Schneider, C. A., Rasband, W. S., and Eliceiri, K. W. (2012) NIH Image to Image J: 25 years of image analysis. *Nat. Methods* **9,** 671–675 CrossRef Medline
49. Huang, D. W., Sherman, B. T., and Lempicki, R. A. (2009) Bioinformatics enrichment tools: Paths toward the comprehensive functional analysis of large gene lists. *Nucleic Acids Res.* **37,** 1–13 CrossRef Medline